Chapter 5

The Dynamics of Dry, Microscopic Granular Chains

In the previous chapter, we established a set of empirical equations of motion for the particles in a groove. In this chapter, we describe the dynamic response of one-dimensional chains of particles in contact in response to a mechanical impulse excitation. The particles tested for this analysis are made of stainless steel 316 and stainless steel 440c (see Table 2.1); all particles have a diameter of 300 micrometers. The rest of this chapter is organized as follows: in section 5.1, we discuss the modeling approach that is used in the analysis and the results that are obtained with it, predicting the propagation of solitary waves. In section 5.2, we present the measured properties of the stress waves that are propagating through these systems (including their group velocity) and amplitude decay. In section 5.3, we discuss the dynamic response of non-ideal particle chains and study the influence of defects (i.e., the presence of inter-particle gaps) in the measured response of micro-granular chains. In section 5.4, we summarize the findings.

5.1. Modeling solitary waves in micro-granular chains

We model the system of micro-particles assuming Hertzian contact interactions and free boundary conditions, using the empirical equations of motion of a free-moving particle that were obtained in the previous chapter. Accordingly, we can describe the motion of the i[th] particle in the chain as:

$$\begin{aligned} & m\,\ddot{z}_i = -sign\left(\dot{z}_i - sR\dot{\theta}_i\right)mg\mu_{pg}/\mathrm{s} - \mathrm{m}(\dot{z}_i/T_0 - \dot{z}_i{}^2/\mathrm{L}) + f_{i-1,i}(z_{i-1}, z_i) - \\ & f_{i,i+1}(z_i, z_{i+1}), \\ & I\ddot{\theta}_i = \mathrm{R}(sign\left(\dot{z}_i - sR\dot{\theta}_i\right)mg\mu_{pg} - sign\left(\dot{\theta_{i-1}} + \dot{\theta}_i\right)f_{i-1,i}(z_{i-1}, z_i)\mu_{pp} \pm \\ & sign\left(\dot{\theta}_i + \dot{\theta_{i+1}}\right)f_{i,i+1}(z_i, z_{i+1})\mu_{pp}), \end{aligned} \tag{5.1}$$

where z_i is the coordinate of the i[th] particles, and $f_{i-1,i}(z_{i-1}, z_i)$ is the Hertzian contact force between the (i-1)[th] and i[th] particles. In Eq. (5.1), $T = 0.052\ s$, $L = 2.5\ mm$, $\mu_{pg} = 0.293$, and $\mu_{pp} = 1.4$ are the empirical parameters obtained in Chapter 4. By using a fourth-order Runge–Kutta solver with a 1 ns time step to solve this equation of motion numerically, we simulate the dynamics of granular chains composed of 15 stainless steel 440c particles with a radius of 150 μm that are resting on a v-

groove (i.e., the micro-granular chain we constructed experimentally; see the next section). The particles are in a close-packed condition with zero pre-compression. We are interested in finding the relationship between the striker velocity and the propagating wave group velocity, to compare the numerical results with the continuum theory derived for highly nonlinear systems [3] (as described in Chapter 1). The solution of the system of equations of motion shows that for a perfectly packed system, the stress waves propagate through the chain forming a solitary wave; this is similar to what has been reported for macroscopic granular systems [36]. An example of the evolution of the particle velocity in time for all 15 particles in the chain as computed numerically is shown in Fig. 5.1a. For these results, the micro-granular chain was excited with an initial striker velocity of 0.1 m/s. It can be seen that when the particles are in close contact, the maximum velocity reached by the particles is about 2/3 of the striker velocity. We perform further numerical simulations to examine the dependency between the maximum particle velocity and the initial striker velocity; the results are shown in Fig. 5.1b. We find a linear relationship between the maximum particle velocity and the striker velocity, $v_{max} = 0.64 v_{striker}$. In Fig. 5.1c, we show the calculated group velocities (red dots) for the propagating stress wave at different initial striker velocities. For comparison, in this figure we also plot the solution of Eq. (1.4), which is the analytical solution derived by Nesterenko for a granular chain that is interacting with only Hertzian force (no rotational degrees of freedom) [2]. By substituting $v_{max} = 0.64 v_{striker}$ from fitting the data in Fig. 5.1b, we have $v_g = \sqrt[5]{\frac{16}{25}} c^{4/5} {v_{max}}^{1/5} = \sqrt[5]{\frac{16}{25}} c^{4/5} (0.64 v_{striker})^{1/5}$. The corresponding (blue) curve in Fig. 5.1c matches the simulation results very well, despite the absence of rotational degrees of freedom in the Nesterenko theory. These results are in line with the analysis of macroscopic granular chains as described in Chapter 1 and in [2].

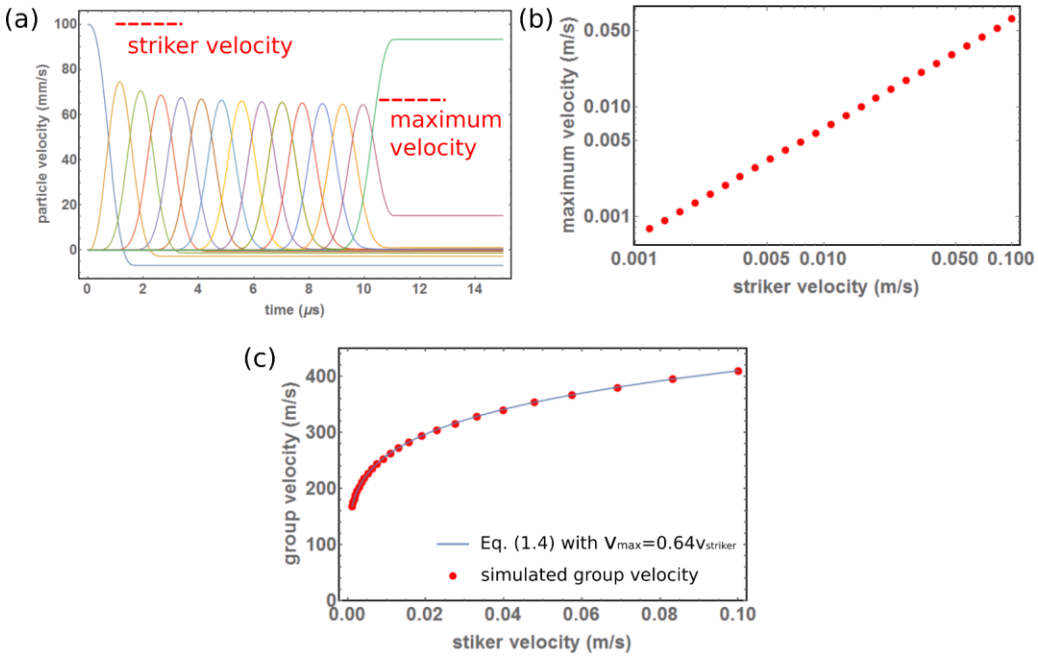

Figure 5.1: Numerically computed nonlinear waves traveling in an uncompressed, micro-granular chain that consists of 15 stainless steel particles (440c) with a radius of 150 μm. The first particle (the striker) has an initial velocity of 0.1 m/s. (a) Velocities of micro-particles along the chain. The solitary wave is seen to evolve to a stable shape after traveling through the first few particles. (b) Calculated maximum particle velocity at different initial striker velocities. The results can be fitted with a linear relation, $v_{max}\sim 0.64 v_s$. (c) Calculated group velocities (red dots) at different initial striker velocities. The results match with the analytical solution for a granular chain (Eq. (1.4) if the $v_{max}\sim 0.64 v_s$ obtained in (c) is assumed.

The agreement between the two models (Eq. 1.4 and Eq. 5.1) might be surprising at first, but it can be understood by estimating the energy transfer to the rotational degrees of freedom (due to the presence of Coulomb friction in our model) and the energy loss that results from dissipation (due to air friction). The ratio between the energy transfer/loss can be estimated with

$$\Delta E^{(Coulomb)}/E \sim -mg\mu_{pg}\Delta x/\frac{1}{2}m{v_{striker}}^2 \sim 2g\mu_{pg}\Delta x/{v_{striker}}^2, \tag{5.2}$$

and

$$\Delta E^{(air\ friction)}/E \sim \frac{1}{2}m{v_{striker}}^2\left(\exp\left(-\frac{2\Delta t}{T}\right)-1\right)/\frac{1}{2}m{v_{striker}}^2 \sim -\frac{2\Delta t}{T}, \tag{5.3}$$

where Δx is the total traveling distance of all particles and Δt is the total interaction time. In the case presented in Fig. 5.1a, we have $\Delta x \sim 2\,\mu m$, $\Delta t \sim 10\,\mu s$, and $\frac{\Delta E^{(Coulomb)}}{E} \sim$ 0.1%, $\frac{\Delta E^{(air\ friction)}}{E} \sim$0.05%. These ratios are both very small compared to the total kinetic energy of the system. From an experimental point of view, a difference of 0.1% or 0.05% is well below the accuracy of the measurements and cannot be directly observed.

The solitary waves observed in the simulations have a temporal width of about 2 μs, which is challenging from an experimental point of view. To correctly resolve the pulse profile experimentally, we need a sampling bandwidth that is greater than 5 MHz. This requirement exceeds the bandwidth of our laser vibrometers (which are limited to operating up to 2.5 MHz). As a consequence, we expect the shape of the measured waveform to be distorted. However, in order to extract useful information from experiments and compare the experimental data with the theoretical models available, we measure the time evolution of the maximum particle velocity, which is not expected to be affected by the limited bandwidth. In the experiments, we measure the velocities of the 2nd and 13th particles in the chain and define their maximum velocities as $v_{max,1} \equiv v_{max,2\mathrm{nd}}$, $v_{max,2} \equiv v_{max,13\mathrm{th}}$. We compare these with the corresponding values obtained in numerical simulations. From our numerical simulations we obtain:

$$v_{max,2}{}^{(simulation)} = 0.72 v_{max,1}{}^{(simulation)},$$

$$v_{max,1}{}^{(simulation)} = 0.89 v_{striker}{}^{(simulation)},$$

$$v_{max,2}{}^{(simulation)} = 0.64 v_{striker}{}^{(simulation)}.$$

In the next section, we compare these numerical results with the corresponding values obtained experimentally.

5.2. Wave propagation in micro-granular chains

To perform experimental measurements of wave propagation in micro-granular chains, we excite the first particle of an assembled micro-granular chain with the laser ablation system, which provides a controlled initial momentum. We measure the propagation of waves along the chain at selected particle locations using two laser vibrometers. To ensure precise excitations, the laser focus needs to be aimed very accurately on the striker. Poor laser excitation alignment results in particles gaining

velocity components in unwanted direction and results in the scattering or buckling of the constructed micro-granular chains.

We measure the time-dependent velocity profiles of the 2nd and 13th particles in the chain, as described in Chapter 2. A typical measurement obtained by the two vibrometers is shown in Fig. 5.2a.

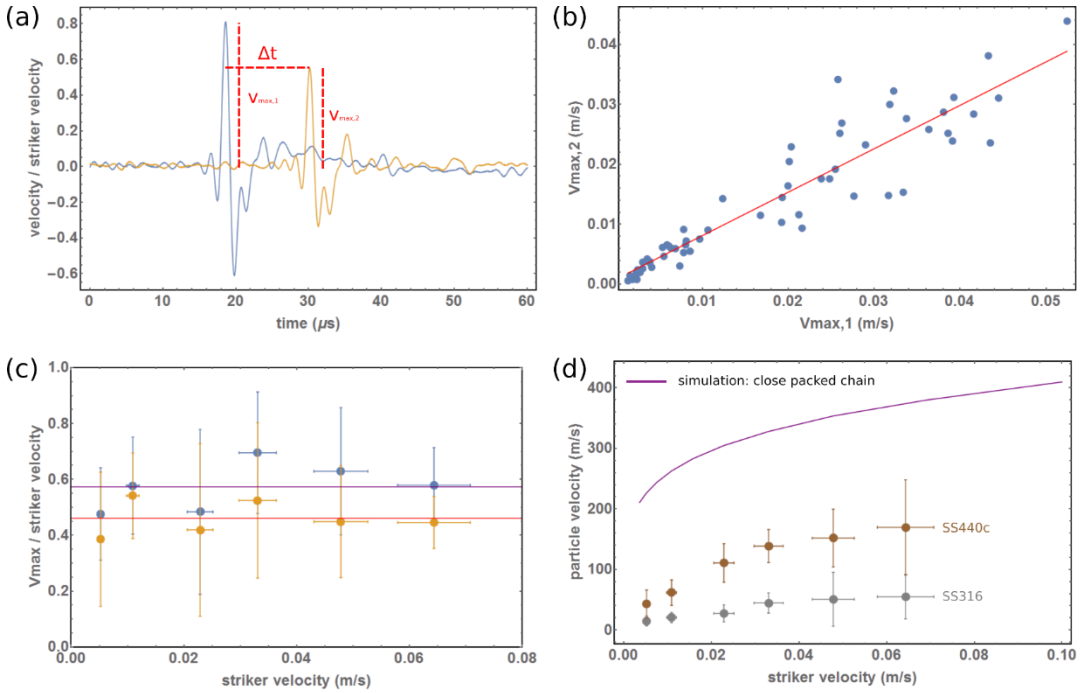

Figure 5.2: Measured particle velocities in a micro-granular chain of 15 stainless steel 440c particles (a) Measured particle velocities (rescaled with the calibration Eq. 2.1 and normalized by the striker velocities) for the 2nd and 13th particles in the chain. From these data we obtain the maximum particle velocities, $v_{max,1}$ and $v_{max,2}$, and the time delay Δt. (b) Measured maximum velocities (red dots) of the two monitored particles. The red fitting line has a slope of 0.80 ± 0.08 (95% confidence interval). (c) Measured maximum velocities (normalized to the striker velocity). An averaging gives $v_{max,1}/v_{striker} = 0.57 \pm 0.09$ and $v_{max,2}/v_{striker} = 0.46 \pm 0.07$ (95% confidence interval). (d) Measured group velocities at different striker velocities.

A typical measurement obtained by the two vibrometers is shown in Fig. 5.2a. The measured vibration is a filtered pulse response function (which is not representative of the real pulse shape because of the bandwidth limits). From this data, a reconstruction of the original waveform shape is difficult. To overcome this issue, as mentioned in the previous section we extract from the vibrometer data only the maximum values of the wave velocities and make no analysis or consideration of the shape and/or

frequency content of the propagating waves. We measure the maximum amplitudes, $v_{max,1}$ and $v_{max,2}$, of the two velocities output by the 2nd and 13th particles and time delays between the maximum amplitudes Δt. We plot the measured $v_{max,1}$ and $v_{max,2}$ in Fig. 5.2b. Despite the large variation of the measured velocities, $v_{max,1}$ and $v_{max,2}$ show a linear dependency and are fitted to obtain their experimental ratio of $v_{max,2}/v_{max,1} = 0.80 \pm 0.08$ (95% confidence interval). This result has a good agreement to the simulation results, ${v_{max,2}}^{(simulation)}/{v_{max,1}}^{(simulation)} = 0.72$. It might seem counter-intuitive that the experimentally obtained ratio between $v_{max,2}$ and $v_{max,1}$ is bigger than the one obtained through simulation, as we know for a perfect Nesterenko granular chain, the maximum velocities decay slightly as the wave propagates (see Fig. 5.1a). We also expect that any energy loss due to imperfection of the experimental system should only contribute to further decreasing the value of $v_{max,2}$. This interesting observation is explained in the next section, where the presence of gaps between particles is considered.

In Fig. 5.2c, we plot the measured $v_{max,1}$, $v_{max,2}$ at different striker velocities; the $v_{max,1}$, $v_{max,2}$ shown are normalized to $v_{striker}$. We have averaged the values of $v_{max,1} = (0.57 \pm 0.09)v_{striker}$ and $v_{max,2} = (0.46 \pm 0.07)v_{striker}$. The predicted values obtained in numerical simulations are ${v_{max,1}}^{(simulation)} = 0.89{v_{striker}}^{(simulation)}$ and ${v_{max,2}}^{(simulation)} = 0.64{v_{striker}}^{(simulation)}$. It seems that the measured values are about 40% smaller than the simulation, which might be a result of extra-loss on the striker due to imperfections in the construction of the chain.

Next we plot the measured group velocity $v_g = (13 - 2)2R/\Delta t$ at varying striker velocities in Fig. 5.2d for both 316 and 440c stainless steel particles. We first see the (striker) velocity. The measured pulse shown in Fig. 5.4a is a filtered response function that is not representative of the real traveling pulse shape, because of the bandwidth limits of our laser acquisition system (as discussed above). From these experimental data, a reconstruction of the original waveform shape is difficult. To overcome this issue, we extract from the vibrometer data only the maximum values of the particle velocities and the time delays between them, Δt, as these values are not affected by the bandwidth limit. We do not analyze the shape and/or frequency content of the propagating waves. We plot the measured $v_{max,1}$ and $v_{max,2}$ in Fig. 5.2b. Despite the large variation of the measured velocities $v_{max,1}$ and $v_{max,2}$ it is possible to fit the data with a linear dependence. The experimental ratio is $v_{max,2}/v_{max,1} = 0.80 \pm 0.08$ (95% confidence interval). This result has a good agreement to the simulation results, ${v_{max,2}}^{(simulation)}/{v_{max,1}}^{(simulation)} = 0.72$. It might seem counter-intuitive

that the experimentally obtained ratio between $v_{max,2}$ and $v_{max,1}$ is bigger than the one obtained through simulation, as we know for a perfect Nesterenko granular chain, the maximum velocities decay slightly as the wave propagates (see Fig. 5.1a). We also expect that any energy loss due to imperfections in the experimental system should only contribute to further decreasing the value of $v_{max,2}$. This interesting observation is explained in the next section, where the presence of gaps between particles is considered.

Finally, we plot the measured group velocity $v_g = (13-2)2R/\Delta t$ at varying striker velocities in Fig. 5.2d for both 316 and 440c stainless steel particles. Remarkably, the propagating wave group velocity varies as a function of the striker velocity for both particles tested. This is a clear indication of the nonlinear interaction between the particles. From the data, however, we note a significant deviation of the group velocities from their predicted values to much lower values. This is again puzzling, since in previous plots we have observed a good agreement between the maximum velocities of the 2nd and 13th particles in the chains. It is surprising that the group velocities can deviate significantly, while the model accurately captures the maximum velocities. In order to explain this phenomenon, we analyze the effects of defects (i.e., gaps) in the chain and discuss the results in the next section.

5.3. Gaps in micro-granular chains

In order to explain the large deviation of the measured group velocity from the group velocity that was calculated with our numerical model for an ideal chain of particles that are perfectly in contact, we must consider the role of defects and gaps between particles in wave propagation. To compute these effects numerically, we include the presence of gaps between the micro-particles in our simulation (Fig. 5.3a). We perform numerical simulations of the wave propagation in a granular chain with randomly distributed gaps between neighboring particles. As seen in Fig. 5.3b, when an average gap of 20 nm is included between each contact, the maximum particle velocity along the chain begins to oscillate (the particle velocity no longer decreases uniformly along the chain), and the oscillation amplitude has a variation of about 20%. This can explain the variations of $v_{max,1}$ and $v_{max,2}$ in the experimental data shown in previous section.

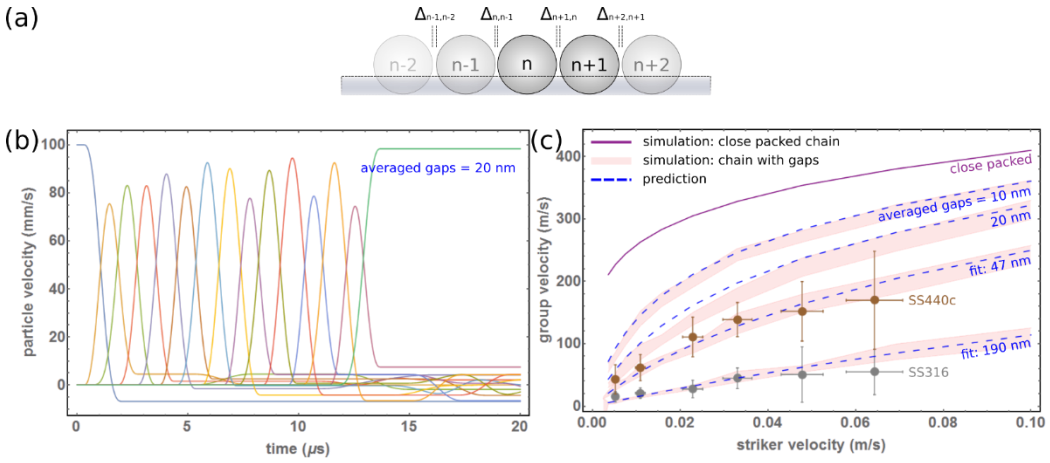

Figure 5.3: Wave propagation in micro-granular chains with gaps. (a) Schematic diagram of the setup obtained by assigning a random gap between neighboring particles. (b) Numerical simulations for waves propagating in a granular chain with gaps. The initial velocity is 0.1 m/s and the average gap size is 20 nm (c) Group velocity as a function of the striker velocity, at various gap sizes. Purple line: simulation of an ideal chain (gap=0). Pink bands: simulation results with randomly generated gap distributions, at a fixed average gap size ranging from 10 to 190 nm. Dashed lines: theoretical predictions obtained with Eq. (26), based on the group velocity of a close-packed chain. The measured group velocity is fitted with the simulation results (dashed lines) of systems with averaged gap = 190 and 47 nm for stainless steel 316 and 440c, respectively.

We then calculate the value of the average group velocity as a function of the striker velocity and compare the results with the experimental data obtained for the two types of particles. The average group velocity is now defined as $v_g = 11(2R + \bar{\Delta})/\Delta t$, where $\bar{\Delta}$ is the average gap size per contact along the chain. The randomly sampled group velocities, at different values of $\bar{\Delta}$, are shown as the pink bands in Fig. 5.3c. We use a simple equation to estimate the measured group velocity:

$$\frac{2R+\bar{\Delta}}{v_g(measurement,with\ gaps)} = \frac{2R}{v_g(simulation,no\ gaps)} + \frac{\bar{\Delta}}{v_{striker}}, \tag{5.4}$$

This formula assumes that the total time of flight is equal to the sum of the time required for a wave to travel through the particles and the time required for the free-moving particles to travel the distance of a gap to reach the neighboring particles. The estimated curves obtained from Eq. (5.4) for different gap sizes are plotted by the blue dashed lines in Fig. 5.3c. We can see that the blue dashed lines lie above the corresponding randomly sampled chains, which is because $v_{striker}$ is not the exact velocity of the free-moving particle, but the highest possible velocity of any particle within the system. The

resulting group velocity therefore defines the upper bound for a chain with randomly distributed gaps, in which the real velocity is lower than $v_{striker}$. These results show that even the presence of very little gaps can significantly alter wave propagation through micro-granular chains. For example, even gaps of only 20 nm (a value that is smaller than 0.1% of the diameter of the particles) can reduce the group velocity of the system by about 1/3. This results from the three order of magnitudes of difference between the group and striker velocities.

We further analyze the experimental data obtained with the close-packed stainless steel 316 and 440c particles. By fitting the experimental points in Fig. 5.3c with different average gap sizes, we show that numerical predictions estimate an average gap size of 190.4 nm in a chain of stainless steel 316 spheres and an average gap size of 47 nm for the chain of 440c particles. Note that the fitting curve lies above the experimental data because we fit it as an upper bound to the data points.

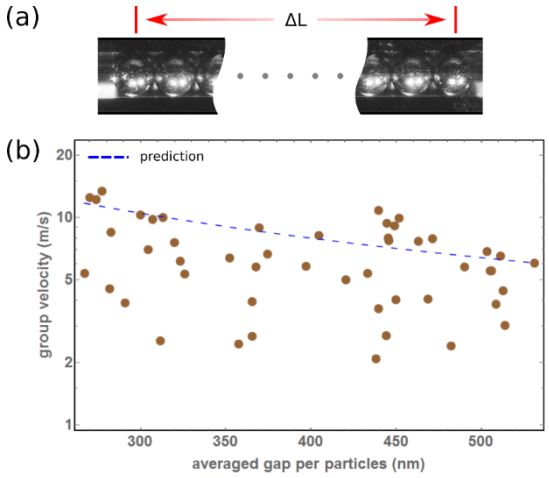

Figure 5.4: Experimental data of group velocity at different gap sizes. The chains are excited with an initial velocity of 0.01m/s and group velocities are measured on a loosely packed chain. (a) Measurement of the total length of the chain. (b) Experimental data for the group velocity (brown dots) and predictions (dashed line). The data are scattered but remain below the upper bound of the dashed line.

Experimentally, no direct way is available for resolving and measuring nanometer-size gaps in a given chain. To further analyze the effect of the gaps in experiments, we intentionally create micro-granular chains with a controlled length (defining an upper bound for the gaps). We create "loosely packed" chains, with a total length that is equal to the length of the ideally packed chain plus 4 to 8 μm. The total length L of each chain is measured with the microscope system. We use $(\Delta L - 11 \times 2R)/11$ to

estimate the average gap size within each chain. We then excite the chains with the striker particle with a fixed striker velocity of 0.1 m/s and measure the resulting group velocities. The results are shown in Fig. 5.4. The numerically predicted curve for the corresponding group velocity is plotted with a dashed line, while the experimental data of the measured group velocities are indicated by brown dots. The measured group velocity appears to be scattered but is generally below the predicted upper bound of the dashed line, which is expected from Eq. (5.4).

5.4. Summary

In this chapter, we experimentally investigated the wave propagation within a one-dimensional chain of micro-particles. We constructed the micro-granular chain with a carefully engineered micro-manipulator system and measured the traveling wave within the chain at different initial striker velocities. We obtained good agreement of propagation amplitude with simulation, but we observed a disagreement in the measured group velocities. This deviation is later explained with the presence of gaps within the non-compressed chain. Further simulation and experiments are then performed to quantify the influence of the gaps on the group velocity.